COMMUNICATION

Enhanced Coupling Through π-Stacking in Imidazole-Based Molecular Junctions

Received 00th January 20xx,
Accepted 00th January 20xx

DOI: 10.1039/x0xx00000x

Tianren Fu,[a] Shanelle Smith,[b] María Camarasa-Gómez,[c] Xiaofang Yu,[b] Jiayi Xue,[b,d] Colin Nuckolls,[a*] Ferdinand Evers,[c*] Latha Venkataraman,[a,e*] Sujun Wei[b*]

We demonstrate that imidazole based π-π stacked dimers form strong and efficient conductance pathways in single-molecule junctions using the scanning-tunneling microscope-break junction (STM-BJ) technique and with density functional theory-based calculations. We first characterize an imidazole-gold contact by measuring the conductance of imidazolyl-terminated alkanes (im-*N*-im, *N* = 3–6). We show that the conductance of these alkanes decays exponentially with increasing length, indicating that the mechanism for electron transport is through tunneling or super-exchange. We also reveal that π-π stacked dimers can be formed between imidazoles and have better coupling than through-bond tunneling. These experimental results are rationalized by calculations of the molecular junction transmission using non-equilibrium Green's function formalism. This study verifies the capability of imidazole as a Au-binding ligand to form stable single- and π-stacked molecule junctions at room temperature.

Imidazole is an aromatic five-member-ring structure with two nitrogen atoms, one pyridine-like and one pyrrole-like nitrogen (N-3 and N-1 as shown in Figure 1). The lone pair electrons on the pyridine-nitrogen coordinates with metals or with protons. Additionally, the electron-rich characteristic of imidazole also enables versatile intermolecular non-covalent interactions, such as accepting hydrogen bond or enhancing π-π interactions. Imidazole thus has varied functionality. For example, as a functional group of the amino acid histidine, it is the active binding site in superoxide dismutases[1, 2]; it also acts as a Brønsted base in serine endopeptidases[3]. In metal organic frameworks (MOFs), it is used as a bidentate but non-chelating ligand[4]. Despite these broad functionalities, the electronic characteristics of imidazole as a Au-binding ligand has not yet been tested.

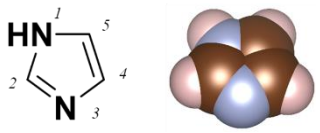

Figure 1. The molecular structure of imidazole, and IUPAC numbering of atoms

Here, we applied the scanning tunneling microscope-based break-junction (STM-BJ) method to create and characterize imidazole-based molecular junctions[5, 6]. We synthesized four imidazole-terminated alkane molecules with an 1,ω-di(imidazol-1-yl)alkanes (**im-3-im**, **im-4-im**, **im-5-im** and **im-6-im**) chemical structure, as shown in Figure 2a. The synthesis is detailed in the supplementary information (SI).

STM-BJ measurements are conducted under ambient condition at room temperature as has been described before[5]. Junctions are formed between a Au substrate and tip from a ~1 mM solution of the target molecule in 1,2,4-trichlorobenzene (TCB). Each individual measurement starts by smashing the tip into the substrate to create a Au-Au contact. The tip is then withdrawn while the conductance, (current/voltage), is measured as a function of the relative tip/substrate displacement and this is repeated at least 5000 times for each molecule. The individual traces are compiled into logarithmically binned conductance histograms.[7]

Figure 2b shows 1D conductance histograms for all four molecules. 2D conductance-displacement histograms are shown in SI Figure S1. All measurements are performed at a 900 mV bias. Note that the bias does not affect conductance for these molecules (see SI Figure S2). A clear peak at ~1 G_0 ($G_0 = 2e^2/h$, the conductance quantum) is seen due to the reproducible formation of a single atom Au contact. The molecular junction conductance peaks occur over a range of 10^{-4} to 10^{-6} G_0 and show a decreasing conductance with increasing

[a] *Department of Chemistry, Columbia University, New York, New York 10027, USA.*
[b] *Department of Chemistry, Queensborough Community College of the City University of New York, Bayside, New York 11364, USA.*
[c] *Institute of Theoretical Physics, University of Regensburg, 93040 Regensburg, Germany.*
[d] *Department of Chemistry and Biochemistry, Queens College of the City University of New York, Flushing, New York 11367, USA.*
[e] *Department of Applied Physics, Columbia University, New York, New York 10027, USA.*

† Footnotes relating to the title and/or authors should appear here.
Electronic Supplementary Information (ESI) available: [details of any supplementary information available should be included here]. See DOI: 10.1039/x0xx00000x

backbone length. This can be attributed to a ballistic tunneling transmission through molecular junction. In addition, for every histogram, there is a broad feature at around 10^{-3} G_0 which we attribute to an intermolecular π-π stacked complex that we will discuss in detail further below[8-13]. Further inspection of the molecular conductance peak reveals that it is actually two peaks, similar to what is observed for pyridine-based linkers[14-16]. Since the imidazole linker is binding to Au with its pyridine-nitrogen, it can form a vertical, primarily σ-coupled junction (left) or a tilted σ- and π-coupled junction (right) as illustrated in the inset of Figure 2c. As the differences between these two binding configurations has been investigated in detail for pyridine linkers before[16, 17], in the following discussion, we will focus primarily on the lower-conducting σ-coupled configuration.

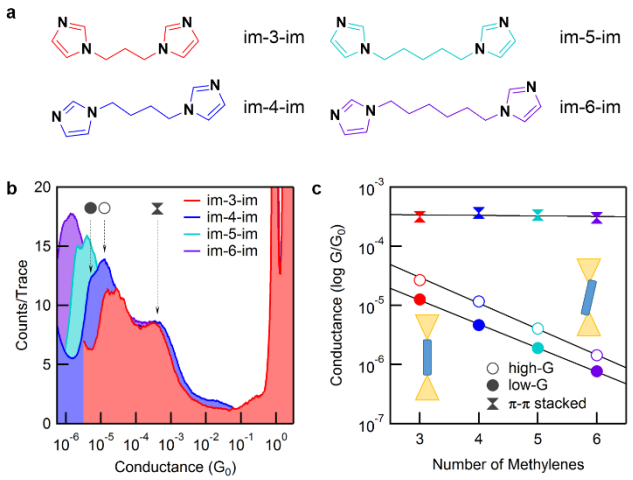

Figure 2. (a) The chemical structures of **im-*N*-im** molecules. (b) Logarithmically-binned conductance histograms (100 bins per decade) for all four molecules generated from 15000 traces each. The three peaks, two that change with the molecular backbone length and one that is independent of the backbone length are indicated by the arrows for **im-4-im**. Histograms are terminated at the noise floor. (c) Molecular junction conductance, determined from a Gaussian fit, is plotted against the number of methylene units in the backbone. The β values determined from the fit are 0.93 (low-*G*) and 1.01 (high-*G*), per methylene.

Figure 2c plots the peak conductance value of each molecule against molecular length. The solid circles represent the conductance of the σ-coupled configuration with a lower-conductance (low-*G*), and the hollow circles represent the conductance of the tilted configuration (high-*G*). Both series show an exponential decay in conductance with increasing molecular length. We fit these experimental data with tunneling transmission model: $G_N = Ae^{-\beta N}$, and obtain a decay constant, β = 0.93 and 1.01 per methylene for the low-*G* and high-*G* configurations respectively. This β value agrees with measurements of alkyl molecules with other linkers[18, 19], and confirms that these follow a tunneling mechanism. By extending the fit to $N = 0$, we estimate the conductance of a molecule with no carbon bridging the two imidazole groups; the inverse of this conductance serves as a metric for the linker contact resistance. For the imidazole linker, we obtain a contact resistance of 65 MΩ for the low-*G* series. As a comparison, the contact resistance for some other common linkers are: -SMe: 0.27 MΩ, -NH_2: 0.37 MΩ and -PMe_2: 0.13 MΩ[18]. We can also compare imidazole with pyridine which has a contact resistance of 23 MΩ as determined from a direct measurement of 4,4'-bipyridine[15]. Although clearly larger than small linkers, imidazole is comparable to pyridine.

We now turn to transport calculations based on density functional theory (DFT), and compute the electronic transmission through Au-**im-*N*-im**-Au junction models. We employ the FHI-aims package[20, 21] with a PBE exchange-correlation functional[22] and apply a non-equilibrium Green's function formalism implemented within AITRANSS package[23, 24]. The structure of a low-G **im-4-im** junction is shown in Figure 3a, using the VESTA program[25]. Each electrode consists of a pyramidal cluster of 55 Au atoms, arranged in 6 layers in the (111) direction with closest interatomic distance of 2.88 Å. The **im-*N*-im** molecules are in fully relaxed in an all *anti* conformation in gas phase and imidazole is bound to the apex atom of Au electrode in a vertical geometry, a structure that represents the lower conducting junction.

The transmission function for all four molecules studied are similar as shown in Figure 3b. The transmission at Fermi (E_F) has a strong contribution from the molecular HOMO-4 and HOMO-2 based σ-channels that decay across the molecular backbone, as can be seen from the isosurface plots for **im-4-im** shown in Figure 3c (the structures in blue frame). The transmission peak at around –1.6 eV relative to E_F (on the occupied side) represents transmission through the molecular HOMO-8 which is also primarily a σ-based orbital (the structure in green frame). The transmission peak at around +2.3 eV relative to E_F results from the weakly coupled π-based molecular LUMO (the structure in orange frame). The transmission at the E_F decreases exponentially with increasing molecular length, in agreement with the experimental results. The calculated conductance values, obtained by applying the Landauer formula to the transmission at E_F, are plotted against the molecular length in the inset of Figure 3b. The calculations overestimate conductance due to known errors with DFT[26] which in turn can also alter the calculated β value. We find that the calculated β value is 1.10/methylene, slightly higher than the experimental one.

We now turn to the molecular conductance peak seen around 10^{-3} G_0 for all the molecules in this series as shown in Figure 2b. We attribute this peak to junctions formed by an intermolecular π-π stacked dimer, (see Figure 4a and 4b). Such a π-π stacked dimer has been observed in aniline derivatives where the contribution of the N-p_z orbital is significant to enhance the intermolecular interaction[27]. The pyrrole nitrogen on the imidazole ring can play a similar role enhancing the electron density in the imidazole π system and augmenting π-π interactions. To confirm this hypothesis, we measure the conductance of 1-methylimidazole (**im-1**) which has only one Au-binding site. The 1D histogram from STM-BJ measurements of **im-1** is shown in Figure 4c, together with the histogram of **im-4-im**. **Im-1** gives a single peak at ~10^{-3} G_0 that overlaps with the peak also observed for all **im-*N*-im** molecules.

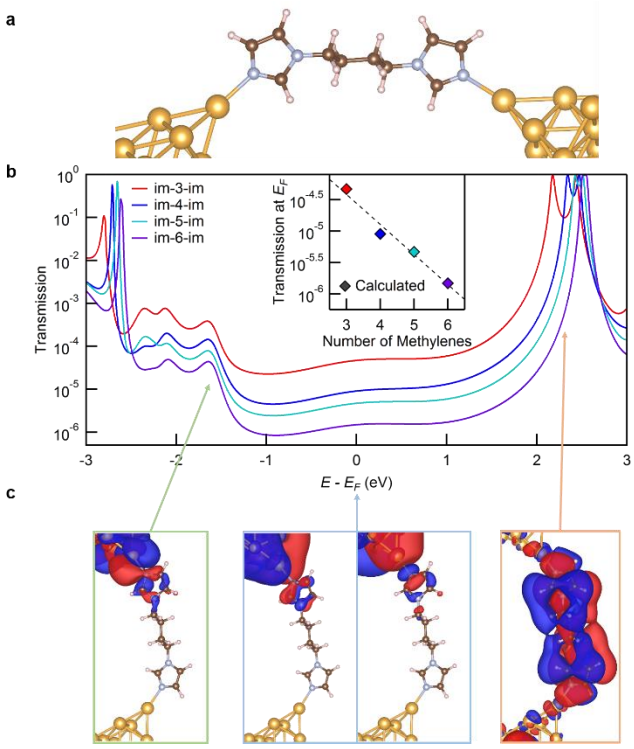

Figure 3. (a) The junction geometry of **im-4-im**. (b) The calculated transmission functions of all the four molecules. Inset: Linear fit of transmission at Fermi energy of each molecular junction. (c) The scattering states for the **im-4-im** junction determined at the Fermi energy and at the energies corresponding to the two peaks closest to the Fermi energy, as indicated in the figure.

Since **im-1** has only one Au-binding site, it can only form a π-π stacked junction. We therefore use flicker noise measurements, which have been used to distinguishes through-space transmission from that of through-bond[28] to confirm this hypothesis. Flicker noise measurements are conducted by first forming an **im-1** dimer junction, holding this for 150 ms and analyzing the conductance, measured with a 100 kHz bandwidth. Two quantities are calculated from the conductance data while the junction is held: the average conductance (G), and the normalized noise power in the form of power spectrum density (PSD). The PSD is obtained from the square of the integral of the discrete Fourier transform of the measured conductance between 100 Hz to 1000 Hz. The lower frequency limit is constrained by the mechanical stability of the setup. The upper limit is determined by the input noise of the current amplifier. Using these quantities, we create 2D histograms of the normalized noise power against the average conductance from 8556 traces. The relation between noise power and conductance is extracted by determining the scaling exponent (N) for which PSD/G^N and G are not correlated. We have previously shown that the relationship between flicker noise PSD and conductance G follows a power law dependence (PSD ~ G^N) with the exponent N being indicative of the electronic coupling type. N close to 2 indicates a through-space coupled molecular junction, while an exponent N of 1 indicates a through-bond coupling. Figure 4d shows the 2D histogram of PSD/G against G where a clear positive correlation is visible. For **im-1**, the correlation between PSD/G^N and G goes to zero when N = 1.9. This is a clear indication to a through-space transmission. We can therefore attribute the conductance peak at around 10^{-3} G_0 to one that involves a through-space coupled intermolecular imidazole dimer.

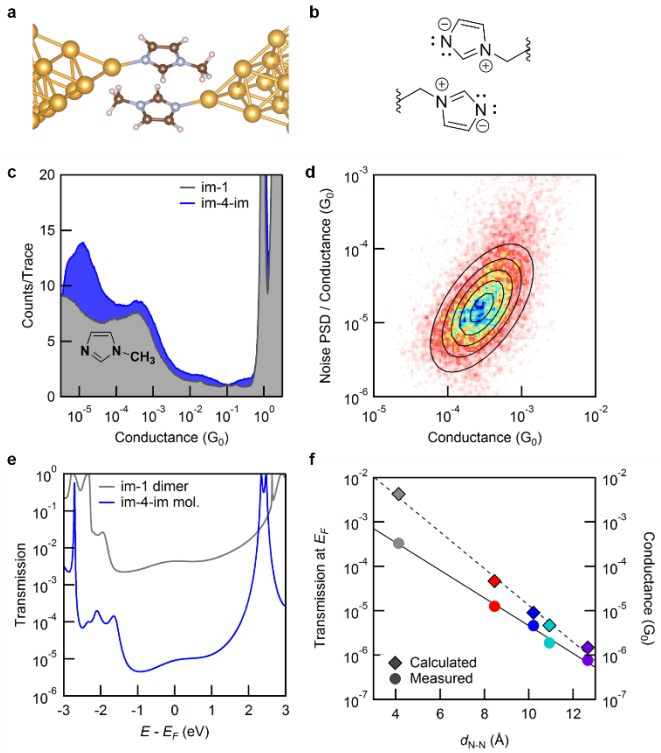

Figure 4. (a) The structure of a π-π stacked 1-methylimidazole (**im-1**) dimer junction used in the DFT calculations. (b) The charge-separated resonance state that stabilizes the π-π stacked dimer. (c) Logarithmically-binned conductance histogram for **im-1** and **im-4-im** measurements. (d) Two-dimensional histogram of PSD/G against the average junction conductance G. (e) Calculated transmission functions of an **im-1** dimer junction along with that of the molecular **im-4-im** junction. (f) The transmission at Fermi of **im-1**, together with **im-*N*-im** plotted against the junction N-N distance (left axis). The corresponding experimental data is also shown (right axis).

To compare this to the calculated transmission, we model the junction as illustrated in Figure 4a; the geometry is optimized within DFT including van der Waals interactions following the methods developed by Tkatchenko and Scheffler[29]. We find that the DFT-relaxed structure has the two **im-1** molecules separated by a ~3.3 Å gap and stabilized by 0.41 eV when compared to two isolated molecules. For the imidazole ring, an electron-rich pyrrole nitrogen and an electron-withdrawing pyridine nitrogen increase the dominance of its charge-separated resonance structure shown in Figure 4b. Thus, imidazole π-π stacked dimer is more strongly bound than benzene dimer (which is stabilized by only 0.15 eV). The transmission across this junction is shown in Figure 4e. At E_F, the transmission of the dimer **im-1** is ~100 times that of the molecular **im-4-im** junction, in agreement with experiment. For the π-π stacked dimer junction of **im-4-im**, the calculated transmission is close to that of dimer **im-1** junction (see

Supplementary Information). The results here confirm that the conductance peaks around 10^{-3} G_0 in Figure 2b arise from intermolecular π-π stacked dimer junctions as shown in Figure 4b, and thus the length of alkyl chain in **im-*N*-im** series is not important. In Figure 4f, we plot the transmission at E_F and the measured conductance against the calculated through-space distance between the two imidazole nitrogens that are directly bound to Au atoms. Interestingly, although the two electrodes are not bridged by one molecule, the π-π stacked dimer structure can still give roughly a same conductance as a single-molecule junction of similar length, in contrast to what is typically expected for such weakly coupled systems[30].

In summary, we have investigated the ability of imidazole to function as an aurophilic linker for molecular junctions using the STM-BJ technique. We find that the conductance of four imidazole-terminated alkanes have a β value that is consistent with that found for other linkers. This provides an outlook to direct measurement on the electronic properties of some imidazole-containing biologically relevant systems. Importantly, we also demonstrated that imidazole can form stable π-π stacked dimers that have a relatively high through-space conductance, which therefore function as the smallest functional group forming stable π-π stacked dimers.

Conflicts of interest

There are no conflicts to declare.

Acknowledgements

M.C.-G. thanks D. Hernangómez-Pérez for fruitful discussions. We acknowledge financial support from the National Science Foundation under award grant CHE-1764256. S.W. thanks the Professional Staff Congress of the City University of New York (PSC-CUNY) Research Award Program (PSC-CUNY Award #60261-00 48) for funding. X.Y., J.X. and S.W. acknowledge support from the CUNY Research Scholars Program, the US Department of Education Minority Science and Engineering Improvement Program (Award #P120A140057) and the National Institute of Health Bridges to the Baccalaureate Program (Award # 5R25GM065096). M.C.-G. and F. E. are grateful for the financial support from the German Research Foundation through the Collaborative Research Center (SFB) 1277 (project B01) and the Research Training Group (GRK) 1570. We thank CUNY Queens College NMR Director Dr. Gopal Subramaniam for assistance.

Notes and references

1. S. V. Antonyuk, R. W. Strange, S. L. Marklund and S. S. Hasnain, *J. Mol. Biol.*, 2009, **388**, 310-326.
2. J. A. Tainer, E. D. Getzoff, J. S. Richardson and D. C. Richardson, *Nature*, 1983, **306**, 284-287.
3. L. Polgar, *Cell Mol. Life Sci.*, 2005, **62**, 2161-2172.
4. K. S. Park, Z. Ni, A. P. Cote, J. Y. Choi, R. D. Huang, F. J. Uribe-Romo, H. K. Chae, M. O'Keeffe and O. M. Yaghi, *P Natl Acad Sci USA*, 2006, **103**, 10186-10191.
5. L. Venkataraman, J. E. Klare, I. W. Tam, C. Nuckolls, M. S. Hybertsen and M. L. Steigerwald, *Nano Lett.*, 2006, **6**, 458 - 462.
6. B. Q. Xu and N. J. Tao, *Science*, 2003, **301**, 1221-1223.
7. M. T. Gonzalez, S. M. Wu, R. Huber, S. J. van der Molen, C. Schonenberger and M. Calame, *Nano Lett.*, 2006, **6**, 2238-2242.
8. S. M. Wu, M. T. Gonzalez, R. Huber, S. Grunder, M. Mayor, C. Schonenberger and M. Calame, *Nat. Nanotechnol.*, 2008, **3**, 569-574.
9. S. Martin, I. Grace, M. R. Bryce, C. S. Wang, R. Jitchati, A. S. Batsanov, S. J. Higgins, C. J. Lambert and R. J. Nichols, *J. Am. Chem. Soc.*, 2010, **132**, 9157-9164.
10. K. Yoshida, I. V. Pobelov, D. Z. Manrique, T. Pope, G. Mészáros, M. Gulcur, M. R. Bryce, C. J. Lambert and T. Wandlowski, *Sci. Rep.*, 2015, **5**, 9002.
11. M. T. González, E. Leary, R. García, P. Verma, M. Á. Herranz, G. Rubio-Bollinger, N. Martín and N. Agraït, *J. Phys. Chem. C*, 2011, **115**, 17973-17978.
12. W. Hong, H. Valkenier, G. Mészáros, D. Z. Manrique, A. Mishchenko, A. Putz, P. M. García, C. J. Lambert, J. C. Hummelen and T. Wandlowski, *Beilstein J. Nanotechnol.*, 2011, **2**, 699-713.
13. J.-T. Zheng, R.-W. Yan, J.-H. Tian, J.-Y. Liu, L.-Q. Pei, D.-Y. Wu, K. Dai, Y. Yang, S. Jin, W. Hong and Z.-Q. Tian, *Electrochimica Acta*, 2016, **200**, 268-275.
14. A. Borges, E. D. Fung, F. Ng, L. Venkataraman and G. C. Solomon, *J. Phys. Chem. Lett.*, 2016, **7**, 4825-4829.
15. M. Kamenetska, S. Y. Quek, A. C. Whalley, M. L. Steigerwald, H. J. Choi, S. G. Louie, C. Nuckolls, M. S. Hybertsen, J. B. Neaton and L. Venkataraman, *J Am Chem Soc*, 2010, **132**, 6817-6821.
16. T. Kim, P. Darancet, J. R. Widawsky, M. Kotiuga, S. Y. Quek, J. B. Neaton and L. Venkataraman, *Nano. Lett.*, 2014, **14**, 794-798.
17. S. Y. Quek, M. Kamenetska, M. L. Steigerwald, H. J. Choi, S. G. Louie, M. S. Hybertsen, J. B. Neaton and L. Venkataraman, *Nat. Nanotechnol.*, 2009, **4**, 230-234.
18. Y. S. Park, A. C. Whalley, M. Kamenetska, M. L. Steigerwald, M. S. Hybertsen, C. Nuckolls and L. Venkataraman, *J. Am. Chem. Soc.*, 2007, **129**, 15768-15769.
19. C. Li, I. Pobelov, T. Wandlowski, A. Bagrets, A. Arnold and F. Evers, *J. Am. Chem. Soc.*, 2008, **130**, 318-326.
20. V. Blum, R. Gehrke, F. Hanke, P. Havu, V. Havu, X. Ren, K. Reuter and M. Scheffler, *Computer Physics Communications*, 2009, **180**, 2175-2196.
21. V. Havu, V. Blum, P. Havu and M. Scheffler, *J. Comp. Phys.*, 2009, **228**, 8367-8379.
22. J. P. Perdew, K. Burke and M. Ernzerhof, *Phys. Rev. Lett.*, 1996, **77**, 3865-3868.
23. A. Arnold, F. Weigend and F. Evers, *J. Chem. Phys.*, 2007, **126**, 174101.
24. A. Bagrets, *J. Chem. Theory Comput.*, 2013, **9**, 2801-2815.
25. K. Momma and F. Izumi, *J. Appl. Cryst.*, 2011, **44**, 1272-1276.
26. M. Koentopp, K. Burke and F. Evers, *Phys. Rev. B*, 2006, **73**, 121403.
27. A. Magyarkuti, O. Adak, A. Halbritter and L. Venkataraman, *Nanoscale*, 2018, **10**, 3362-3368.
28. O. Adak, E. Rosenthal, J. Meisner, E. F. Andrade, A. N. Pasupathy, C. Nuckolls, M. S. Hybertsen and L. Venkataraman, *Nano Lett.*, 2015, **15**, 4143-4149.
29. A. Tkatchenko and M. Scheffler, *Phys. Rev. Lett.*, 2009, **102**, 73005-73005.

30. R. Frisenda, V. A. Janssen, F. C. Grozema, H. S. van der Zant and N. Renaud, *Nat. Chem.*, 2016, **8**, 1099-1104.